



COFS: COntrollable Furniture layout Synthesis

Wamiq Reyaz Para
wamiq.para@kaust.edu.sa
KAUST
Saudi Arabia

Paul Guerrero
guerrero@adobe.com
Adobe Research
UK

Niloy J. Mitra
nimitra@adobe.com
University College London and Adobe Research
UK

Peter Wonka
pwonka@gmail.com
KAUST
Saudi Arabia

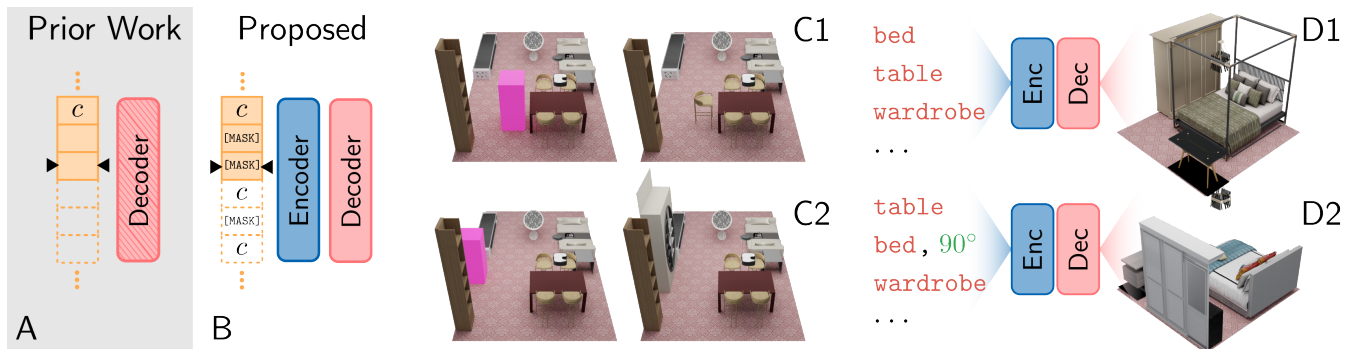


Figure 1: (A) Current autoregressive layout generators provide limited user-control over the generated results, since any generated value (denoted by black triangles) in the sequence representation of a layout can only be conditioned on values c that occur earlier in the sequence. (B) We propose COFS, a layout generator with an encoder-decoder architecture that allows all values in the sequence to be given as condition. This enables conditioning a generated layout on an arbitrary subset of objects or object attributes, which is impossible with current autoregressive layout generators. (C1, C2) Only the position of an object, shown as pink cuboid, is given as a condition, and COFS performs context-aware generation of the remaining attributes, such as object type and orientation. (D1) Only object types are provided as condition. (D2) Bed orientation is added to the condition. Note how the layout adapts to fit the updated condition.

ABSTRACT

Realistic, scalable, and controllable generation of furniture layouts is essential for many applications in virtual reality, augmented reality, game development and synthetic data generation. The most successful current methods tackle this problem as a sequence generation problem which imposes a specific ordering on the elements of the layout, making it hard to exert fine-grained control over the attributes of a generated scene. Existing methods provide control through *object-level conditioning*, or scene completion, where generation can be conditioned on an arbitrary subset of furniture objects. However, *attribute-level conditioning*, where generation can be conditioned on an arbitrary subset of object attributes, is not supported. We propose COFS, a method to generate furniture layouts that enables fine-grained control through attribute-level conditioning. For example, COFS allows specifying only the scale

and type of objects that should be placed in the scene and the generator chooses their positions and orientations; or the position that should be occupied by objects can be specified and the generator chooses their type, scale, orientation, etc. Our results show both qualitatively and quantitatively that we significantly outperform existing methods on attribute-level conditioning.

CCS CONCEPTS

• Computing methodologies → Shape modeling.

KEYWORDS

Furniture layout, transformers, conditional generation



This work is licensed under a Creative Commons Attribution International 4.0 License.

SIGGRAPH '23 Conference Proceedings, August 06–10, 2023, Los Angeles, CA, USA
© 2023 Copyright held by the owner/author(s).
ACM ISBN 979-8-4007-0159-7/23/08.
<https://doi.org/10.1145/3588432.3591561>

ACM Reference Format:

Wamiq Reyaz Para, Paul Guerrero, Niloy J. Mitra, and Peter Wonka. 2023. COFS: COntrollable Furniture layout Synthesis. In *Special Interest Group on Computer Graphics and Interactive Techniques Conference Conference Proceedings (SIGGRAPH '23 Conference Proceedings)*, August 06–10, 2023, Los Angeles, CA, USA. ACM, New York, NY, USA, 11 pages. <https://doi.org/10.1145/3588432.3591561>

1 INTRODUCTION

Automatic generation of realistic assets enables content creation at a scale that is not possible with traditional manual workflows. It is driven by the growing demand for virtual assets in both the creative industries, virtual worlds, and increasingly data-hungry deep model training. In the context of automatic asset generation, 3D scene and layout generation plays a central role as much of the demand is for the types of real-world scenes we see and interact with every day, such as building interiors.

Deep generative models for assets like images, videos, 3D shapes, and 3D scenes have come a long way to meet this demand. In the context of 3D scene and layout modeling, in particular autoregressive models based on transformers enjoy great success. Inspired by language modeling, these architectures treat layouts as sequences of tokens that are generated one after the other and typically represent attributes of furniture objects, such as the type, position, or scale of an object. These architectures are particularly well suited for modeling spatial relationships between elements of a layout. For example, [Para et al. 2021] generate two-dimensional interior layouts with two transformers, one for furniture objects and one for spatial constraints between these objects, while SceneFormer [Wang et al. 2021] and ATISS [Paschalidou et al. 2021] extend interior layout generation to 3D.

A key limitation of a basic autoregressive approach is that it only provides limited control over the generated scene. It enforces a sequential generation order, where new tokens can only be conditioned on previously generated tokens and in addition it requires a consistent ordering of the token sequence. This precludes both *object-level conditioning*, where generation is conditioned on a partial scene, e.g., an arbitrary subset of furniture objects, and *attribute-level conditioning*, where generation is conditioned on an arbitrary subset of attributes of the furniture objects, e.g., class or position of target objects. Most recently, ATISS [Paschalidou et al. 2021] partially alleviates this problem by randomly permuting furniture objects during training, effectively enabling *object-level conditioning*. However, attribute-level conditioning still remains elusive.

We aim to improve on these results by enabling attribute-level conditioning, in addition to object-level conditioning. For example, a user might be interested to ask for a room with a table and two chairs, without specifying exactly where these objects should be located. Another example is to perform object queries for given geometry attributes. The user could specify the location of an object and query the most likely class, orientation, and size of an object at the given location. Our model thereby extends the baseline ATISS with new functionality while retaining all its existing properties and performance.

The main technical difficulty in achieving attribute-level conditioning is due to the autoregressive nature of the generative model. Tokens in the sequence that define a scene are generated iteratively, and each step only has information about the previously generated tokens. Thus, the condition can only be given at the start of the sequence, otherwise some generation steps will miss some of the conditioning information. The main idea of our work is to allow for attribute-level conditioning using two mechanisms: (i) Like ATISS, we train our generator to be approximately invariant to object permutations by randomly permuting furniture objects at

training time. This enables object-level conditioning since an arbitrary subset of objects can be given as the start of the sequence. To condition on a partial set of object attributes however, the condition is not restricted to the start of the sequence. Attributes that are given as condition follow unconstrained attributes that need to be generated. (ii) To give our autoregressive model knowledge of the entire conditioning information in each step, we additionally use a transformer encoder that provides cross-attention over the complete conditioning information in each step. These two mechanisms allow us to accurately condition on arbitrary subsets of the token sequence. Our main competitor ATISS [Paschalidou et al. 2021] can only perform object-level conditioning and predicts attributes in a fixed order. Consequently, it cannot partially specify object attributes as a condition (cf. Fig. 10).

In our experiments, we demonstrate four applications: (i) attribute-level conditioning, (ii) attribute-level outlier detection, (iii) object-level conditioning, and (iv) unconditional generation. We compare to three current state-of-the-art layout generation methods [Paschalidou et al. 2021; Ritchie et al. 2019; Wang et al. 2021] and show performance that is on par or superior on unconditional generation and object-level conditioning, while also enabling attribute-level conditioning, which, to the best of our knowledge, is currently not supported by any existing layout generation method.

2 RELATED WORK

We discuss recent work that we draw inspiration from. In particular, we build on previous work in Indoor Scene Synthesis, Masked Language Models, and Set Transformers.

Indoor Scene Synthesis. Before the rise of deep-learning methods, indoor scene synthesis methods relied on layout guidelines developed by skilled interior designers, and an optimization strategy such that the adherence to those guidelines is maximized [Fisher et al. 2012; Weiss et al. 2019; Yu et al. 2011]. Such optimization is usually based on sampling methods like simulated annealing, MCMC, or rjMCMC. Deep learning based methods, e.g. [Paschalidou et al. 2021; Ritchie et al. 2019; Wang et al. 2019, 2021] are substantially faster and can better capture the variability of the design space. The state-of-the-art methods among them are autoregressive in nature. All of these operate on a top-down view of a partially generated scene. PlanIT [Wang et al. 2019] and FastSynth [Ritchie et al. 2019] then autoregressively generate the rest of the scene. FastSynth uses separate CNNs+MLPs to create probability distributions over location, size and orientation and categories. PlanIT on the other hand generates graphs where nodes are objects and edges are constraints on those objects. Then a scene is instantiated by solving a CSP on that graph.

Recent methods, SceneFormer [Wang et al. 2021] and ATISS [Paschalidou et al. 2021] use transformer based architectures to sidestep the problem of rendering a partial scene which makes PlanIT and FastSynth slow. This is because using a transformer allows the model to accumulate information from previously generated objects using the attention mechanism. SceneFormer flattens the scene into a structured sequence of the object attributes, where the objects are ordered lexicographically in terms of their position. It then trains a separate model for each of the attributes. ATISS breaks the requirement of using a specific order by training on all possible

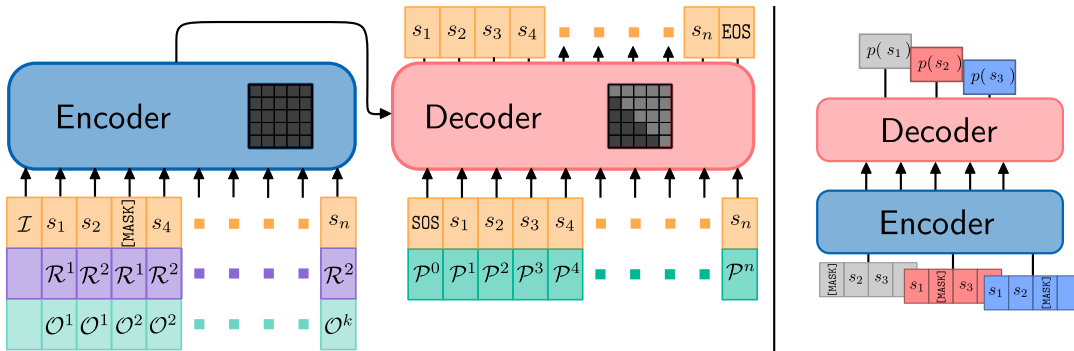


Figure 2: COFS Overview. (Left): We use a BART-like encoder-decoder model, with bidirectional attention in the encoder and an autoregressive decoder. The encoder encodes the layout as a set without ordering information and therefore does not receive (*absolute*) position tokens. However, to disambiguate a single object, the encoder receives additional information in the form of *Relative Position Tokens* \mathcal{R}^i , and the *Object Index Tokens* \mathcal{O}^i . During training, object order is randomly permuted and a random proportion of tokens is replaced with a [MASK] token. The decoder outputs a sequence representation of the set and is trained with *Absolute Position Tokens* \mathcal{P}^i . It performs two tasks - 1. *copy-paste*: the decoder copies the unmasked attributes to their proper location 2. *mask-prediction*: the decoder predicts the actual value of the token corresponding to a [MASK] token in the encoder input. (Right): During inference, we measure the likelihood of a given test set token using an input sequence where only this token is masked out.

permutations of the object order and removing the position encoding. In addition, it uses a single transformer model for all attributes and relies on different decoding heads which makes it substantially faster than other models while also having significantly fewer parameters.

Masked Language Models. Masked Language Models (MLMs) like BERT [Devlin et al. 2019], ROBERTa [Liu et al. 2019], and BART [Lewis et al. 2020] are pretrained on large amounts of unlabeled data in an unsupervised fashion, and are then fine-tuned on a much smaller labeled dataset. These fine-tuned models show impressive performance on their corresponding downstream tasks. However, the generative capability of these models has not been much explored except by Wang et al. in [Wang and Cho 2019], which uses a Gibbs-sampling approach to sample from a pre-trained BERT model. In follow up work, [Mansimov et al. 2020], proposes more general sampling approaches. However, the sample quality is still inferior to autoregressive models like GPT-2 [Radford et al. 2019] and GPT-3 [Brown et al. 2020]. More recently, MLMs have received renewed interest especially in the context of image-generation [Chang et al. 2022; Issenhuth et al. 2021]. MaskGIT [Chang et al. 2022] shows that with a carefully designed masking schedule, high quality image samples can be generated from MLMs with parallel sampling which makes them much faster than autoregressive models. Edi-BERT [Issenhuth et al. 2021] shows that the BERT masking objective can be successfully used with a VQGAN [Esser et al. 2021] representation of an image to perform high quality image editing. Our model resembles BART used as a generative model. Most related to our proposed method is the concurrent work BLT [Kong et al. 2022], where the authors propose a BERT-style decoder-only model. However, they still use a specific ordering amongst attribute types, which restricts the subset of attributes that can be used as condition, unlike our method that does not have such a restriction.

Set Transformers. Zaheer et al. [Zaheer et al. 2017] introduced a framework called DeepSets providing a mathematical foundation for networks operating on set-structured data. A key insight is that operations in the network need to be permutation invariant. Methods based on such a formulation were extremely successful, especially in the context of point-cloud processing [Charles et al. 2017; Ravanbakhsh et al. 2016]. Transformer models without any form of positional encoding are permutation invariant by design. Yet, almost all the groundbreaking works in transformers use some form of positional encoding, as in objection detection [Carion et al. 2020], language generation [Brown et al. 2020; Radford et al. 2019], and image-generation [Chang et al. 2022]. One of the early attempts to use a truly permutation invariant set transformer was in Set Transformer [Lee et al. 2019], who methodically designed principled operations that are permutation invariant but could only achieve respectable performance in toy-problems. However, recent work based on [Lee et al. 2019] shows impressive performance in 3d-Object Detection [Chenheng He and Zhang 2022], 3d Pose Estimation [Ugrinovic et al. 2022], and SFM [Moran et al. 2021].

3 METHOD

Our goal is a generative model of object layouts that allows for both object-level and attribute-level conditioning. Attribute-level conditioning enables flexible partial layout specification, like specifying only the number and types of objects in a layout, but not their positions, or exploring suggestions for plausible objects at given positions in the layout. Figure 2 shows an architecture overview.

3.1 Layout Representation

We focus on 3D layouts in our experiments. A 3D layout $\mathcal{L} = (\mathcal{I}, \mathcal{B})$ is composed of two elements - a top-down representation of the layout boundary \mathcal{I} , such as the walls of a room, and a set of k three-dimensional oriented bounding-boxes $\mathcal{B} = \{B_i\}_{i=1}^k$ of the

objects in the layout. The boundary is given as a binary raster image and each bounding box is represented by four attributes: $B_i = (\tau_i, t_i, e_i, r_i)$, representing the object class, center position, size, and orientation, respectively. The orientation is a rotation about the up-axis, giving a total of 8 scalars per bounding box. The layout is arranged into a sequence S by concatenating all bounding box parameters. Additionally, special start and stop tokens SOS and EOS are added to mark the start and the end of a sequence: $S = [\text{SOS}; B_1; \dots; B_k; \text{EOS}]$, where $[\cdot]$ denotes concatenation. The layout boundary \mathcal{I} is not generated by our method, but it is used as condition, Section 3.3 provides details.

3.2 Generative Model

We use a transformer-based generative model, as these types of generative models have shown great performance in the current state of the art. Originally proposed as a generative model for language, transformer-based generative models represents layouts as a sequence of tokens $S = (s_1, \dots, s_n)$ that are generated auto-regressively; one token is generated at a time, based on all previously generated tokens:

$$p(s_i | S_{<i}) = f_\theta(S_{<i}), \quad (1)$$

where $p(s_i | S_{<i})$ is the probability distribution over the value of token s_i , computed by the generative model f_θ given the previously generated tokens $S_{<i} = (s_1, \dots, s_{i-1})$. We sample from $p(s_i | S_{<i})$ to obtain the token s_i . Each token represents one attribute of an object, and groups of adjacent tokens correspond to objects. More details on the layout representation are described in Section 3.1.

Limitations of traditional conditioning. To condition a transformer-based generative model on a partial sequence $C = (c_0, \dots, c_m)$, we can replace tokens of S with the corresponding tokens of C , giving us the sequence S^C . This is done after each generation step, so that the probability for the token in each step is conditioned on $S_{<i}^C$ instead of $S_{<i}$:

$$p(s_i^C | S_{<i}^C) = f_\theta(S_{<i}^C). \quad (2)$$

Each generated token s_i^C in S^C (i.e. tokens that are not replaced by tokens in C) needs to have knowledge of the full condition during its generation step, otherwise the generated value may be incompatible with some part of the condition. Therefore, since each generated token s_i only has information about the partial sequence $S_{<i}^C$ of tokens that are closer to the start of the sequence, the condition can only be given as start of the sequence:

$$s_i^C = \begin{cases} c_i & \text{if } i \leq |C| \\ s_i & \text{otherwise.} \end{cases} \quad (3)$$

Typically both the objects and the attributes of the objects in the sequence are consistently ordered according to some strategy, for example based on a raster order of the object positions [Para et al. 2021], or on the object size [Wang et al. 2019]. Therefore, a generative model $f_\theta^{\text{ordered}}$ that is only trained to generate sequences in that order cannot handle different orderings, so that in general:

$$f_\theta^{\text{ordered}}(S_{<i}^C) \neq f_\theta^{\text{ordered}}(\pi_o(S_{<i}^C)), \quad (4)$$

where π_o is a random permutations of the objects in sequence $S_{<i}$. The consistent ordering improves the performance of the generative

model, but also presents a challenge for conditioning: it limits the information that can appear in the condition. In a bedroom layout, for example, if beds are always generated before nightstands in the consistent ordering, the layout can never be conditioned on nightstands only, as this would preclude the following tokens from containing a bed.

Object-level conditioning. Recent work [Paschalidou et al. 2021] tackles this issue by forgoing the consistent object ordering, and instead training the generator to be approximately invariant to permutations π_o of objects in the sequence:

$$f_\theta(S_{<i}^C) \approx f_\theta(\pi_o(S_{<i}^C)), \quad (5)$$

This makes generation more difficult, but enables object-level conditioning by allowing conditioning on *arbitrary* subset of objects, as now arbitrary objects can appear at the start of the sequence. However, since only objects are permuted and not their attributes, it does not allow conditioning on subsets of object attributes. Permuting object attributes to appear at arbitrary positions in the sequence is not a good solution to enable attribute-level conditioning, as this would make it very hard for the generator to determine which attribute corresponds to which object.

Attribute-level conditioning. We propose to extend previous work to allow for attribute-level conditioning by using two different conditioning mechanisms, in addition to the approximate object permutation invariance: First, similar to previous work, we provide the condition as partial sequence C . However, unlike previous work, some tokens in the condition are unconstrained and will not be used to replace generated tokens. We introduce special mask tokens \mathcal{M} in C to mark these unconstrained tokens. For example, if all tokens corresponding to object positions and orientations in C are mask tokens, the positions and orientations will be generated by our model, only the remaining tokens: object types and sizes will be constrained by the condition. The tokens s_i^C of the constrained sequence S^C are then defined as:

$$s_i^C = \begin{cases} c_i & \text{if } i \leq |C| \text{ and } c_i \neq \mathcal{M} \\ s_i & \text{otherwise.} \end{cases} \quad (6)$$

Second, to provide information about the full condition to each generated token, we modify f_θ to use a transformer encoder g_ϕ that encodes the condition C into a set of feature vectors that each generated token has access to:

$$p(s_i^C | S_{<i}^C, C) = f_\theta(S_{<i}^C, C^\mathcal{G}) \text{ where } C^\mathcal{G} = \{g_\phi(c_1, C), \dots, g_\phi(c_{|C|}, C)\}, \quad (7)$$

where $C^\mathcal{G}$ is the output of the encoder, a set of encoded condition tokens. We use a standard transformer encoder-decoder setup [Vaswani et al. 2017] for f_θ and g_ϕ , implementation details are provided in Section 3.3, and the complete architecture is described in detail in the appendix.

Parameter probability distributions. The generative model outputs a probability distribution over one scalar component of the bounding box parameters in each step. Probability distributions over the discrete object class τ are represented as vectors of logits l_τ over *discrete* choices that can be converted to probabilities with the softmax function. Similar to previous work [Paschalidou

et al. 2021; Salimans et al. 2017], we represent probability distributions over *continuous* parameters, like the center position, size, and orientation, as mixture of T logistic distributions.

$$p(b) = \frac{1}{\sum_i \pi_i} \sum_{i=1}^T \alpha_i \text{Logistic}(\mu_i, \sigma_i), \quad p(\tau) = \text{softmax}(l_\tau), \quad (8)$$

where b is a single scalar attribute from t_i , e_i , or r_i . The mixture weight, mean and variance of the logistic distribution components are denoted as α , μ , σ , respectively. Each probability distribution over a continuous scalar component is parameterized by a $3T$ -dimensional vector, and probability distributions over the object class are represented as n_τ -dimensional vectors, where n_τ is the number of object classes.

3.3 Implementation

Condition encoder g_ϕ . To encode the condition C into a set of encoded condition tokens C^g , we use a Transformer encoder with full bidirectional attention. As positional encoding, we provide two additional sequences: *object index tokens O^i* provide for each token the object index in the permuted sequence of objects; and *relative position tokens R^i* provide for each token the element index inside the attribute tuple of an object. Since the attribute tuples are consistently ordered the index can be used to identify the attribute type of a token. These sequences are used as additional inputs to the encoder. The encoder architecture is based on BART [Lewis et al. 2020], details are provided in the appendix.

Boundary encoder g_ψ^I . To allow conditioning on the layout boundary \mathcal{I} , we prepend a feature vector encoding z_I of the boundary to the input of the condition encoder, as shown in Figure 2, so that the encoder receives both z_I and the condition sequence C . Similar to ATISS, we use an untrained ResNet-18 [He et al. 2016] to encode a top-down view of the layout boundary into an embedding vector.

Generative model f_θ . The generative model is implemented as a Transformer decoder with a causal attention mask. Each block of the decoder performs cross-attention over the encoded condition tokens C^g . As positional encoding, we provide *absolute position tokens \mathcal{P}* , which provide for each token the absolute position in the sequence S . This sequence is used as additional input to the generative model. The output of the generative model in each step is one of the parametric probability distributions described in Eq. 8. Since the probability distributions for discrete and continuous values have a different numbers of parameters, we use a different final linear layer in the generative model for continuous and discrete parameters. Similar to the encoder, the architecture of the generative model is based on BART [Lewis et al. 2020].

Training. During training, we create a ground truth sequence S^{GT} with randomly permuted objects. We generate the condition C as a copy of S^{GT} and mask out a random percentage of the tokens by replacing them with the mask token \mathcal{M} . The boundary encoder g_ψ^I , the condition encoder g_ϕ and the generative model f_θ are then trained jointly, with the task to generate the full sequence S^{GT} . For unmasked tokens in C , this is a copy task from C to the output sequence S . For masked tokens, this is a scene completion task. We

use the negative log-likelihood loss between the predicted probabilities $p(s_i)$ and ground truth values s_i^{GT} for tokens corresponding to continuous parameters, and the cross-entropy loss for the object category τ . The model is trained with teacher-forcing.

Sampling. We generate a sequence auto-regressively, one token at a time, by sampling the probability distribution predicted by the generative model (as defined in Eq. 7) in each step. We use the same model for both conditional and unconditional generation. For unconditional generation, we start with a condition C where all tokens are mask token \mathcal{M} . To provide more complete information about the partially generated layout to the encoded condition tokens C^g , we update the condition C after each generation step by replacing mask tokens with the generated tokens. Empirically, we observed that this improves generation performance. An illustration and the full algorithm of this approach is shown in the supplementary. Once a layout has been generated, we populate the bounding boxes with objects from the dataset with a simple retrieval scheme. For each bounding box, we pick the object of the given category τ that best matches the size of the bounding box. In the supplementary, we present an ablation of the tokens O^i , R^i , and \mathcal{P} that we add to the conditional encoder and generative model.

4 RESULTS

Datasets. We train and evaluate our model on the 3D-FRONT dataset [Fu et al. 2021]. It consists of about 10k indoor furniture layouts created by professional designers. We train on the BEDROOM category and follow ATISS preprocessing which removes a few problematic layouts that have intersections between objects, mislabeled objects, or layouts that have extremely large or small dimensions. For further details on the preprocessing, we refer the reader to ATISS [Paschalidou et al. 2021]. This yields approximately 6k/224, 0.6k/125, 3k/516 and 2.6k/583 total/test set layouts for BEDROOM, LIBRARY, DINING, LIVING, respectively.

Baseline. ATISS [Paschalidou et al. 2021] is the most recent furniture layout generation method that provides the largest amount of control over the generated layout, and is therefore most related to our method. However, ATISS does not provide pretrained models, hence we train their models using the official code¹ matching their training settings as closely as possible. While ATISS does not support attribute-level conditioning, we can still use it as a baseline by applying the sampling procedure defined in Eq. 6: we sample tokens as usual, but when reaching a token that is given as condition (i.e. a token in C that is not a mask token), we replace the sampled value with the value of the condition. ATISS samples the class first, followed by translation, size and orientation.

Note that permuting attributes in ATISS may seem like a straightforward solution for attribute-level conditioning in ATISS. However, this would lead to several unsolved problems: (i) The permuted sequence of attributes would require additional information to determine which attribute corresponds to which scene object. This information would also need to be generated along with the attribute values. It is unclear what form this information should take to work well with the transformer. (ii) Currently, the main transformer in ATISS generates one token per object instead of per

¹<https://github.com/nv-tlabs/atiss>, commit 0cce45b

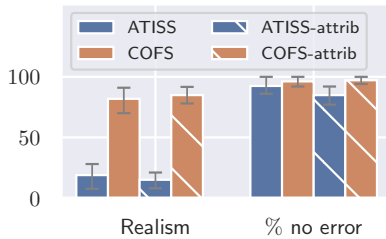


Figure 3: Perceptual Study. We compare the percentage of comparisons in which users found either method more realistic (left), and in which users did not find any obvious errors such as object intersections (right), with 95% confidence intervals as error bars. Results show a large advantage for COFS in realism of layouts generated with attribute-level conditioning (-attrib), and a smaller, but still significant advantage in the percentage of error-free layouts. This advantage is also present in the unconditional setting.

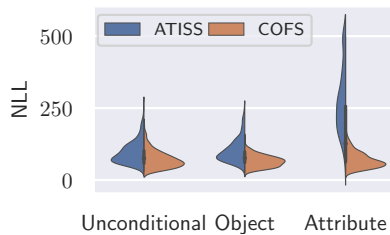


Figure 4: NLL comparison. We compare the NLL of our method to ATISS in three settings: unconditional generation, object-level conditioning, and attribute-level conditioning; all three on layouts from the BEDROOM test set.

attribute, so a significant change to ATISS would be necessary to allow for permuted attribute tokens.

4.1 Perceptual Study

We conducted two perceptual studies to evaluate the quality of generated furniture layouts compared to ATISS. One of the studies focused on unconditionally generated layouts and the other on layouts generated with attribute-level conditioning. For this purpose, we randomly sampled layouts from the BEDROOM layouts evaluated in the previous section for both COFS and ATISS. Subjects were shown a pair of layouts generated from the same floorplan boundary by COFS and ATISS, and asked these questions: which of the layouts looked more realistic, and for each of the two layouts, if it showed obvious errors like intersections. A total of 9 subjects participated in the unconditional study, and 8 subjects participated in the attribute-level study. More details about setup can be found in the supplementary. Figure 3 shows the results. We can see that the our method produces significantly more realistic layouts compared to ATISS. The error plots on the right-hand side show that this only in some part due to avoiding obvious errors such as intersections. These results are further validated in the next section.

4.2 Quantitative Results

Metrics. For *unconditional generation*, we use the negative log-likelihood of test set sequences in our model as main quantitative

metric. A small NLL shows that a model approximates the dataset distribution well. For both *object-level* and *attribute-level* conditioning, we use the NLL of the generated sequences as the metric. The NLL computation includes the condition tokens that come from the test set. If the generated layout does not harmonize with the condition, the NLL will be high.

Choosing conditions. For *object-level* conditioning, we remove three random objects from each test set sequence to obtain condition sequences C . For *attribute-level conditioning*, conditions C are obtained from test set sequences by replacing all tokens except size and position tokens with mask tokens, effectively conditioning on the sizes and positions of all objects, and letting the generator infer the types and orientations of all objects.

Discussion. Figure 4 shows NLL results on the BEDROOM category. For unconditional generation, we can see that we perform on par or slightly better than ATISS. We believe that our slight advantage here might be due a more fine-grained sequence representation of the layout on our side, which allows for more detailed attention. For object-level conditioning, our performance is slightly better than ATISS, again because of detailed attention. Our main contribution, however, lies in attribute-level conditioning, where we can see a clear advantage for our method. Since ATISS cannot look ahead in the sequence, any generated token cannot take into account future condition tokens. The bidirectional attention of our encoder enables look-ahead and gives the generator knowledge of all future condition tokens, giving us generated layouts that can better adapt to the supplied condition.

Constraint Satisfaction. ATISS cannot constrain on future tokens. However, ATISS can still be used to generate constrained layouts by performing rejection-sampling [Gentle 2000].

This means we generate samples unconditionally and discard any samples that do not satisfy our given constraints. This is obviously quite inefficient. In the inset figure, we quantify how inefficient ATISS is in comparison to COFS. The x-axis is the number of constraints we enforce, and the y-axis is the average number of samples needed to satisfy those constraints. This is performed over the whole test set of BEDROOM and the constraints are chosen to be locations of the Ground Truth objects. A sample is considered a success if it is within $\epsilon = 0.01$ of the constraint. We see that for COFS, the number is almost constant regardless of the number of constraints, as the model learns to copy-paste attributes supplied as constraints.

We see that COFS almost always needs a single sample to satisfy the constraints. The number is higher than 1 because of a few reasons - 1. sampling is inherently random and sometimes the samples are produced which are further than the threshold ϵ , 2. L-shaped boundaries sometimes provide strong priors which makes the model ignore the condition. ATISS, on the other struggles as the number of constraints increases. This is expected - with increasing number of constraints, the search space grows exponentially. Overall, our proposed method is many orders of magnitude faster than ATISS for *attribute-level conditioning*, especially when considering timing details as well (cf. Table 1).

4.3 Qualitative Results

A few examples of furniture layouts generated with attribute-level conditioning are shown in Figure 1 and in Figure 5. See the captions for details. Figure 7 additionally shows how attribute-level conditioning can be used to perform sequential edits of a furniture layout.

COFS can be used to generate layouts with some control on the generated attributes (see Discussion, supplementary). We show examples of such control in Fig. 6 where we generate bedroom layouts with control of the bed direction by constraining the bed angle and see that the model generates reasonable layouts. To have more control, we now also constrain to have a dressing-table opposite the bed. COFS generates good layouts for these constraints. ATISS which samples angles after location cannot perform such a task.

4.4 Additional Applications

In addition to attribute-level conditioning, we show that COFS can also be used for the applications proposed by ATISS.

Scene Completion. In Figure 8, we show layouts generated with object-level conditioning, providing the objects shown in the top row as condition. In order to perform this task, the existing object attributes are added to the start of the sequence as condition and the object attributes to be generated are masked. Sampling and replacing each [MASK] token leads to a complete layout. We see that in each example, our method generates a plausible layout.

Outlier Detection. As a second application, we show how to use COFS to perform outlier detection. To estimate the likelihood of a token at position i , we follow [Salazar et al. 2020] and replace the token at i th position with [MASK]. This can be performed in parallel by creating a batch in which only one element is replaced with [MASK]. The likelihood of one object is then the product of likelihoods of all its attributes. Attributes or objects with low likelihood can then be resampled. Results on several of the layout categories of our dataset are shown in Figure 9. This can be thought of as a form of attributed-conditioned generation.

4.5 More Unconditional Generation Experiments

Here we present additional experiments with unconditional generation. We include two additional state-of-the-art methods for unconditional generation, FastSynth [Ritchie et al. 2019] and SceneFormer [Wang et al. 2021], in our quantitative results.

We use a set of metrics that mostly derive from [Paschalidou et al. 2021; Ritchie et al. 2019]. They are defined in greater detail in the supplementary. Following [Ritchie et al. 2019], we report the KL-divergence between the distribution of the classes of generated objects and the distribution of classes of the objects in the test set. We further report the Classification Accuracy Score (CAS) [Paschalidou et al. 2021]. Additionally, we compute the FID by rendering the populated layout from a top-down view using an orthographic camera at a resolution of 256×256 . We report the FID computed between these rendered top down images of sampled layouts and the renders of the ground truth layouts. We also compare the time required to generate a single scene for different categories and the

number of parameters required by each model. Our model requires significantly less time and fewer parameters than existing methods. Slightly over 50% of our parameters come by the ResNet-18 [He et al. 2016] boundary encoder. Thus, our proposed network is very light.

Results are shown in Table 1. The results suggest that overall, COFS performs roughly on par or slightly superior to ATISS, with slightly inferior results in the CAS metric, comparable results in the FID metrics, and more substantially improved results in the KL-divergence metric. Details of these metrics and examples of unconditionally generated layouts are shown in the supplementary.

5 CONCLUSIONS

We proposed a new framework to produce layouts with auto-regressive transformers with arbitrary conditioning information. While previous work was only able to condition on a set of complete objects, we extend this functionality and also allow for conditioning on individual attributes of objects. Our framework thereby enables several new modeling applications that cannot be achieved by any published framework.

Limitations and Future Work. The first limitation of our model is related to our simple object retrieval scheme based only on bounding box sizes. This often leads to stylistically different objects in close proximity even if the bounding box dimensions are only slightly different. We show such an example in the inset. The second is related to the training objective of the model - we only consider the cross entropy/NLL. Thus, the network does not have explicit knowledge of design principles such as non-intersection, or object co-occurrence. This means that the model completely relies on the data being high-quality to ensure such output.



In the supplementary, we highlight the fact that certain scenes in the dataset have problematic layouts, and our method cannot filter them out. We show an example of intersections in the inset (center). Thirdly, the performance on the LIVING and DINING datasets is not as good as the other classes, which is clear from the CAS scores. This is in part because the datasets are small but also have significantly more objects than BEDROOM or LIBRARY. This leads to accumulated errors. We would like to explore novel sampling strategies to mitigate such errors. Lastly, while the conditioning works well, it is not guaranteed to generate a good layout. For example, in the inset (right), we set the condition to be two beds opposite each other, but the network is unable to place them in valid locations. Adding explicit design knowledge would help mitigate such arrangements, but we leave that extension to future work.

ACKNOWLEDGMENTS

This work was supported by the SDAIA-KAUST Center of Excellence in Data Science and Artificial Intelligence (SDAIA-KAUST

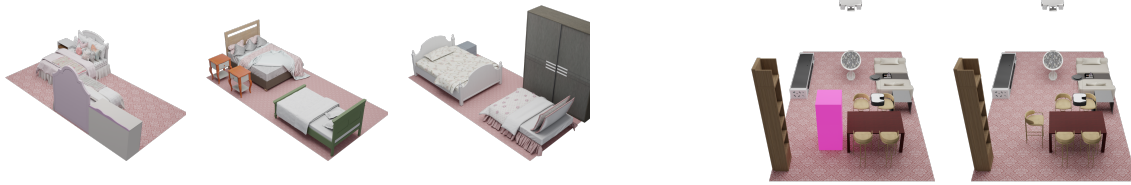


Figure 5: Attribute-level conditioning: On the left, we show a GT floorplan. We set the condition to include two beds facing opposite directions and sample. The model generates two plausible layouts for this challenging case (see supplementary). On the right, we constrain the location of the next object to be sampled. The location is highlighted in pink. In this example, the network automatically infers the proper class and size. The constraints force the inferred size into a narrow range, such that the chair even matches the style of the chairs in the example on the left, even though we use a simple object-retrieval scheme.

Table 1: Comparison on Unconditional Generation: We provide floorplan boundaries from the Ground Truth as an input to the methods and compare the quality of generate layouts. We retrain the ATISS model and report metrics. The retrained model is called ATISS*.

	CAS $\times 10^2$ (\downarrow)				KL-Divergence $\times 10^3$ (\downarrow)				FID (\downarrow)				Synthesis Time (ms) (\downarrow)				Params ($\times 10^6$) (\downarrow)
	BEDROOM	LIVING	DINING	LIBRARY	BEDROOM	LIVING	DINING	LIBRARY	BEDROOM	LIVING	DINING	LIBRARY	BEDROOM	LIVING	DINING	LIBRARY	
FastSynth	88.3	94.5	93.5	81.5	6.4	17.6	51.8	43.1	88.1	66.6	58.9	86.6	13193.77	30578.54	26596.08	10813.87	38.1
SceneFormer	94.5	97.2	94.1	88.0	5.2	31.3	36.8	23.2	90.6	68.1	60.1	89.1	849.37	731.84	901.17	369.74	129.29
ATISS*	61.1	76.4	69.1	61.77	8.6	14.1	15.6	10.1	73.0	43.32	47.66	75.34	102.38	201.59	201.84	88.24	36.05
Ours	61.0	78.9	76.1	66.2	5.0	8.1	9.3	6.7	73.2	35.9	43.12	75.72	33.69	77.37	76.75	29.32	19.44

AI). The authors would also like to acknowledge support from the UCL AI Centre and gifts from Adobe.

REFERENCES

- Tom B. Brown, Benjamin Mann, Nick Ryder, Melanie Subbiah, Jared Kaplan, Prafulla Dhariwal, Arvind Neelakantan, Pranav Shyam, Girish Sastry, Amanda Askell, Sandhini Agarwal, Ariel Herbert-Voss, Gretchen Krueger, Tom Henighan, Rewon Child, Aditya Ramesh, Daniel M. Ziegler, Jeffrey Wu, Clemens Winter, Christopher Hesse, Mark Chen, Eric Sigler, Mateusz Litwin, Scott Gray, Benjamin Chess, Jack Clark, Christopher Berner, Sam McCandlish, Alec Radford, Ilya Sutskever, and Dario Amodei. 2020. Language Models are Few-Shot Learners. (2020). arXiv:2005.14165 [cs.CL]
- Nicolas Carion, Francisco Massa, Gabriel Synnaeve, Nicolas Usunier, Alexander Kirillov, and Sergey Zagoruyko. 2020. End-to-End Object Detection with Transformers. In *ECCV*.
- Huiwen Chang, Han Zhang, Lu Jiang, Ce Liu, and William T. Freeman. 2022. MaskGIT: Masked Generative Image Transformer. In *The IEEE Conference on Computer Vision and Pattern Recognition (CVPR)*.
- R. Qi Charles, Hao Su, Mo Kaichun, and Leonidas J. Guibas. 2017. PointNet: Deep Learning on Point Sets for 3D Classification and Segmentation. In *2017 IEEE Conference on Computer Vision and Pattern Recognition (CVPR)*. 77–85. <https://doi.org/10.1109/CVPR.2017.16>
- Shuai Li Chenhang He, Ruihuang Li and Lei Zhang. 2022. Voxel Set Transformer: A Set-to-Set Approach to 3D Object Detection from Point Clouds. In *Proceedings of the IEEE Conference on Computer Vision and Pattern Recognition*.
- Jacob Devlin, Ming-Wei Chang, Kenton Lee, and Kristina Toutanova. 2019. BERT: Pre-training of Deep Bidirectional Transformers for Language Understanding. In *Proceedings of the 2019 Conference of the North American Chapter of the Association for Computational Linguistics: Human Language Technologies, Volume 1 (Long and Short Papers)*. Association for Computational Linguistics, Minneapolis, Minnesota, 4171–4186. <https://doi.org/10.18653/v1/N19-1423>
- Patrick Esser, Robin Rombach, and Björn Ommer. 2021. Taming Transformers for High-Resolution Image Synthesis. In *2021 IEEE/CVF Conference on Computer Vision and Pattern Recognition (CVPR)*. 12868–12878. <https://doi.org/10.1109/CVPR46437.2021.01268>
- Matthew Fisher, Daniel Ritchie, Manolis Savva, Thomas Funkhouser, and Pat Hanrahan. 2012. Example-Based Synthesis of 3D Object Arrangements. *ACM Trans. Graph.* 31, 6, Article 135 (Nov 2012), 11 pages. <https://doi.org/10.1145/2366145.2366154>
- Huan Fu, Bowen Cai, Lin Gao, Ling-Xiao Zhang, Jiaming Wang, Cao Li, Qixun Zeng, Chengyue Sun, Rongfei Jia, Binqiang Zhao, and Hao Zhang. 2021. 3D-FRONT: 3D Furnished Rooms with layOuts and semaNTics. In *2021 IEEE/CVF International Conference on Computer Vision (ICCV)*. 10913–10922. <https://doi.org/10.1109/ICCV48922.2021.01075>
- James Gentle. 2000. Monte Carlo Statistical Methods by C. P. Robert; G. Casella. *Journal of the Royal Statistical Society. Series D (The Statistician)* 49 (01 2000), 632–633. <https://doi.org/10.2307/2681053>
- Kaiming He, Xiangyu Zhang, Shaoqing Ren, and Jian Sun. 2016. Deep Residual Learning for Image Recognition. In *2016 IEEE Conference on Computer Vision and Pattern Recognition (CVPR)*. 770–778. <https://doi.org/10.1109/CVPR.2016.90>
- Thibaut Issenhuth, Ugo Tanielian, Jérémie Mary, and David Picard. 2021. EdiBERT, a generative model for image editing. *arXiv preprint arXiv:2111.15264* (2021).
- Xiang Kong, Lu Jiang, Huiwen Chang, Han Zhang, Yuan Hao, Haifeng Gong, and Irfan Essa. 2022. BLT: Bidirectional Layout Transformer For Controllable Layout Generation. In *Computer Vision – ECCV 2022: 17th European Conference, Tel Aviv, Israel, October 23–27, 2022, Proceedings, Part XVII* (Tel Aviv, Israel). Springer-Verlag, Berlin, Heidelberg, 474–490. https://doi.org/10.1007/978-3-031-19790-1_29
- Juho Lee, Yoonho Lee, Jungtaek Kim, Adam Kosior, Seungjin Choi, and Yee Whye Teh. 2019. Set Transformer: A Framework for Attention-based Permutation-Invariant Neural Networks. In *Proceedings of the 36th International Conference on Machine Learning*. 3744–3753.
- Mike Lewis, Yinhan Liu, Naman Goyal, Marjan Ghazvininejad, Abdelrahman Mohamed, Omer Levy, Veselin Stoyanov, and Luke Zettlemoyer. 2020. BART: Denoising Sequence-to-Sequence Pre-training for Natural Language Generation, Translation, and Comprehension. In *Proceedings of the 58th Annual Meeting of the Association for Computational Linguistics*. Association for Computational Linguistics, Online, 7871–7880. <https://doi.org/10.18653/v1/2020.acl-main.703>
- Yinhan Liu, Myle Ott, Naman Goyal, Jingfei Du, Mandar Joshi, Danqi Chen, Omer Levy, Mike Lewis, Luke Zettlemoyer, and Veselin Stoyanov. 2019. Roberta: A robustly optimized bert pretraining approach. *arXiv preprint arXiv:1907.11692* (2019).
- Elman Mansimov, Alex Wang, and Kyunghyun Cho. 2020. A Generalized Framework of Sequence Generation with Application to Undirected Sequence Models. <https://openreview.net/forum?id=Bjllbo6VtDH>
- Dror Moran, Hodaya Koslowsky, Yoni Kasten, Haggai Maron, Meirav Galun, and Ronen Basri. 2021. Deep Permutation Equivariant Structure from Motion. In *2021 IEEE/CVF International Conference on Computer Vision (ICCV)*. 5956–5966. <https://doi.org/10.1109/ICCV48922.2021.00592>
- Wamiq Para, Paul Guerrero, Tom Kelly, Leonidas Guibas, and Peter Wonka. 2021. Generative Layout Modeling using Constraint Graphs. In *2021 IEEE/CVF International Conference on Computer Vision (ICCV)*. 6670–6680. <https://doi.org/10.1109/ICCV48922.2021.00662>
- Despoina Paschalidou, Amlan Kar, Maria Shugrina, Karsten Kreis, Andreas Geiger, and Sanja Fidler. 2021. ATISS: Autoregressive Transformers for Indoor Scene Synthesis. In *Advances in Neural Information Processing Systems (NeurIPS)*.
- Alec Radford, Jeff Wu, Rewon Child, David Luan, Dario Amodei, and Ilya Sutskever. 2019. Language Models are Unsupervised Multitask Learners. (2019).
- Siamak Ravanbakhsh, Jeff Schneider, and Barnabas Poczos. 2016. Deep learning with sets and point clouds. *arXiv preprint arXiv:1611.04500* (2016).

- Daniel Ritchie, Kai Wang, and Yu-An Lin. 2019. Fast and Flexible Indoor Scene Synthesis via Deep Convolutional Generative Models. In *2019 IEEE/CVF Conference on Computer Vision and Pattern Recognition (CVPR)*. 6175–6183. <https://doi.org/10.1109/CVPR.2019.00634>
- Julian Salazar, Davis Liang, Toan Q. Nguyen, and Katrin Kirchhoff. 2020. Masked Language Model Scoring. In *Proceedings of the 58th Annual Meeting of the Association for Computational Linguistics*. Association for Computational Linguistics, Online, 2699–2712. <https://doi.org/10.18653/v1/2020.acl-main.240>
- Tim Salimans, Andrej Karpathy, Xi Chen, and Diederik P. Kingma. 2017. PixelCNN++: A PixelCNN Implementation with Discretized Logistic Mixture Likelihood and Other Modifications. In *ICLR*.
- Nicolas Ugrinovic, Adria Ruiz, Antonio Agudo, Alberto Sanfeliu, and Francesc Moreno-Noguer. 2022. Permutation-Invariant Relational Network for Multi-person 3D Pose Estimation. *arXiv preprint arXiv:2204.04913* (2022).
- Ashish Vaswani, Noam Shazeer, Niki Parmar, Jakob Uszkoreit, Llion Jones, Aidan N. Gomez, Lukasz Kaiser, and Illia Polosukhin. 2017. Attention is All You Need. In *Proceedings of the 31st International Conference on Neural Information Processing Systems* (Long Beach, California, USA) (*NIPS'17*). Curran Associates Inc., Red Hook, NY, USA, 6000–6010.
- Alex Wang and Kyunghyun Cho. 2019. Bert has a mouth, and it must speak: Bert as a markov random field language model. *arXiv preprint arXiv:1902.04094* (2019).
- Kai Wang, Yu-An Lin, Ben Weissmann, Manolis Savva, Angel X. Chang, and Daniel Ritchie. 2019. PlanIT: Planning and Instantiating Indoor Scenes with Relation Graph and Spatial Prior Networks. *ACM Trans. Graph.* 38, 4, Article 132 (jul 2019), 15 pages. <https://doi.org/10.1145/3306346.3322941>
- Xinpeng Wang, Chandan Yeshwanth, and Matthias Nießner. 2021. Sceneformer: Indoor scene generation with transformers. In *2021 International Conference on 3D Vision (3DV)*. IEEE, 106–115.
- Tomer Weiss, Alan Litteneker, Noah Duncan, Masaki Nakada, Chenfanfu Jiang, Lap-Fai Yu, and Demetri Terzopoulos. 2019. Fast and Scalable Position-Based Layout Synthesis. *IEEE Transactions on Visualization and Computer Graphics* 25, 12 (2019), 3231–3243. <https://doi.org/10.1109/TVCG.2018.2866436>
- Lap-Fai Yu, Sai-Kit Yeung, Chi-Keung Tang, Demetri Terzopoulos, Tony F. Chan, and Stanley J. Osher. 2011. Make It Home: Automatic Optimization of Furniture Arrangement. *ACM Trans. Graph.* 30, 4, Article 86 (Jul 2011), 12 pages. <https://doi.org/10.1145/2010324.1964981>
- Manzil Zaheer, Satwik Kottur, Siamak Ravanbakhsh, Barnabas Poczos, Ruslan R Salakhutdinov, and Alexander J Smola. 2017. Deep Sets. In *Advances in Neural Information Processing Systems 30*, I. Guyon, U. V. Luxburg, S. Bengio, H. Wallach, R. Fergus, S. Vishwanathan, and R. Garnett (Eds.). Curran Associates, Inc., 3391–3401. <http://papers.nips.cc/paper/6931-deep-sets.pdf>



Figure 6: Fine-grained conditioning: GT is on the left. In the middle two columns, we constrain the first class to be bed, and set a constraint on the angle of the bed, and see that the rest of the layout arranges to fit the constraints. In the next two columns, we constrain the layout to contain a dressing-table at an angle opposite to the bed. The dressing-tables are highlighted.

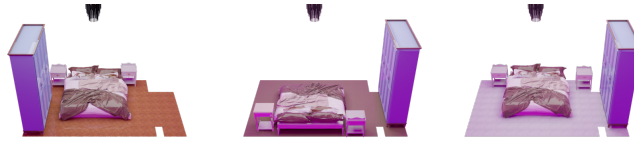


Figure 7: Sequential edits with attribute-level conditioning: We show how COFS can be used to selectively edit parts of a scene. Left shows GT and the other two are samples with classes and orientation as condition. When we change orientation of a few objects (bed, nightstand and wardrobe first, then only bed and nightstand), COFS produces realistic layouts affecting only a part of the scene. More details in the supplementary.



Figure 8: Object-level conditioning. In the top row, we show examples of object-level conditions that were used to condition generation of the scenes shown below. The generated layouts all plausibly combine the generated objects with the objects given as condition into realistic layouts.

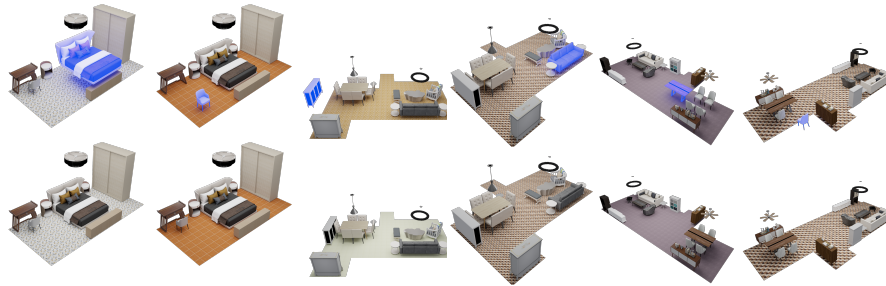


Figure 9: Outlier detection: Our model can utilize bidirectional attention to reason about unlikely arrangements of furniture. We can then sample new attributes that create a more likely layout. In contrast, ATISS can only sample whole objects. Top row: An object is perturbed to create an outlier (highlighted in blue). Bottom row: The object can be identified by its low likelihood, and new attributes sampled which place it more naturally.

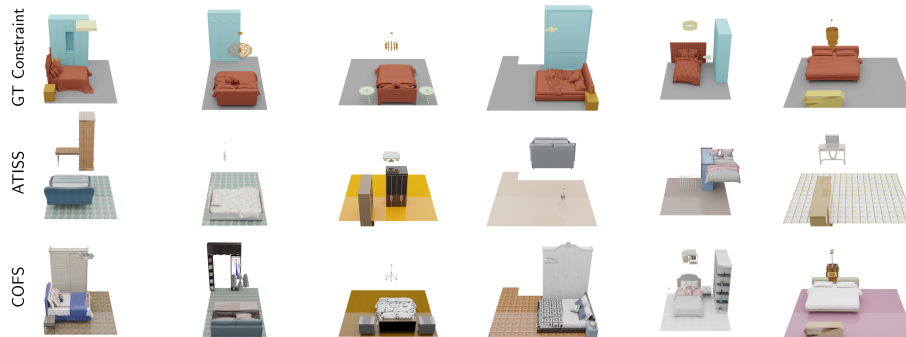


Figure 10: Conditioning on the future: We condition the models on GT locations and sizes and predict rotation and angles. As ATISS can only sample location after class, the baseline method of Section 4 produces bad layouts. COFS on the other hand is able to reconstruct the GT layout closely.